IN-ROLL STRESS ANALYSIS CONSIDERING AIR-ENTRAINMENT AT THE ROLL-INLET WITH THE EFFECT OF GROOVES ON NIP ROLL SURFACE

by

M. Sasaki[1], K. Kohno[1], K. Tanimoto[1], S. Takahashi[1],
S. Suzuki[1], and H. Hashimoto[2]
[1]Mitsubishi Heavy Industries, Ltd.
[2]Tokai University
JAPAN

ABSTRACT

High-speed winding of paper web sometimes leads the winding system into unstable states, interlayer slippage of wound roll, paper breakage and so on, due to the excessive air-entrainment at the roll-inlet of nip contact region. These phenomena are more frequently observed on coated paper or plastic film comparing with newspaper, because the former allows little permeation of air and their surface roughness is small. Therefore, it is of vital importance to clarify the in-roll stress of wound roll considering the effect of air-entrainment.

Generally, it is known that the amount of air-entrainment is affected by grooving shape of nip roll surface. In this paper, we focused on the grooving shape and investigated the relationship with the air-entrainment into two rolls being pressed each other and the grooving shape in order to achieve stable winding at high speed. We conducted experiments using small sized test machine. Entrained air-film thickness was evaluated applying the solution of the elasto-hydrodynamic lubrication for foil bearing with the consideration of nip profile at the grooved area. Air film thickness was measured to ensure the applicability of the above theory.

Consequently, we found that the air film thickness can be estimated considering the effect of grooves on the nip roll surface, and that the validity of the above estimations was ensured from experimental investigations. Furthermore, it became to be able to propose the optimal shape of grooves on nip roll surface to maintain the stable winding at high speed and at large-diameter in reel.

NOMENCLATURES

b	Nip contact half width
C_{eq}	Equivalent Compliance of two cylinders pressed each other
d_0	Groove depth
$d(z)$	profile of groove depth (Cross direction)
E_r	Young modulus of rolls in radial direction (Cross direction)

E_z	Young modulus of web in axial direction
E_θ	Young modulus of web in circumferential direction (Machine direction)
h	Air film thickness
N	Nip load
p	Air pressure
R_d	Radius of reel drum
R_{eq}	Equivalent radius of two cylinders
R_g	Radius of shallow groove
R_q	RMS surface roughness
R_r	Radius of wound roll
R_w	Curvature radius of web in non-contact area at the nip region
T	Web tension
t	Web thickness
V	Winding speed
W	Roll width
w_g	Width of shallow groove
w_l	Length of flat area of shallow groove
w_p	Groove pitch
Δw_g	Non-contact groove width at the nip region
β	Coefficient of permeance of a paper web per unit period and unit pressure difference
δ_0	Deformation of roll at the nip region
μ	Viscosity of air
μ_{st}	Static frictional coefficient
ν	Poisson's ratio
$\theta(z)$	Angular position of groove
σ_r	Radial stress of wound roll

INTRODUCTION

With the increasing demands for high productivity in paper machine mills, there are demands for higher performance of paper winding systems in terms of higher winding speed, wider paper width and larger wound roll diameters. However, high-speed winding of paper web sometimes leads the winding system into unstable states, lateral slide, wrinkle, interlayer slippage of wound roll and so on, due to the excessive air-entrainment in the wound roll. These phenomena are frequently observed in handling coated paper or plastic film comparing with newspaper, because the former allows little permeation of air and their surface roughness is small. Therefore, it is of vital importance to clarify the in-roll stress of wound roll considering the effect of air-entrainment.

So far, in-roll stress fields of wound rolls have been investigated experimentally and theoretically by many precursors to clarify the influences of winding parameters. Altmann's [1] or Hakiel's [2] theories are well known as the basic winding model and widely used academically and practically. These numerical models have been assured and modified by many researchers. Authors [3, 4] also extended the Hakiel's model and proposed the numerical formulation for estimating the in-roll stress of wound roll taking account of nonlineality in web compressibility, air-entrainment and permeance. They made sure of the significant effect of air-entrainment and permeance upon the in-roll stress by experimental and theoretical investigations. In addition, authors [5] made sure that center winding and grooved reel drum was effective to maintain web tension for stable winding with coated paper from the relationship between the frictional force and the air film thickness at the nip region. The frictional force at that region was derived with consideration of "effective" frictional coefficient proposed by Good [6] and

Hashimoto [7]. The numerical evaluation of air-entrainment was derived from the theories for foil bearing. Chang [8] had applied it to the winding model to demonstrate the significant effect of winding speed, nip load and stiffness of wound roll.

For evaluating the in-roll stress distribution of practical wound rolls, however, it is indispensable to clarify the air-entrainment considering the effect of grooves on nip roll surface, because the grooving shape have significant effect on the air-entrainment into wound rolls.

In this paper, we investigated the relationship with the air-entrainment into two rolls being pressed each other and the shape of grooves on nip roll surface and we conducted experiments using small sized test machine. Entrained air-film thickness was evaluated applying the solution of the elasto-hydrodynamic lubrication for foil bearing with the consideration of elastic deformation of wound roll at the grooved area. Air film thickness was measured to ensure the applicability of the above theory.

Subsequently, in-roll stress was analyzed considering the effect of grooving shape and winding tests with coated paper were conducted in order to assure the applicability of proposed theory by usage of our pilot reel under the operating conditions of 2000m/min in winding speed.

THEORY

Background and outline

Fig. 1 shows the typical winding system. Generally, two types of grooving are used for high-speed winding with coated paper. One is called vent groove and other is called shallow groove. Fig. 2 shows the typical grooving shape on nip roll surface, which is combined with vent and shallow grooves.

It is known that both types of grooving are used to prevent air bags from building in winding system. Fig. 3 shows the effect of grooves on nip roll surface. Vent grooves prevent incoming web to float from nip roll surface and shallow grooves prevent the entrained air in wound roll to being blocked at the nip.

Shallow grooves, however, can cause the increase in the amount of air-entrainment at the roll inlet and lead the serious roll defect if grooving depth or width is oversized. On the other hands, the amount of air-entrainment at the nip remains nearly unaffected by vent grooves because the grooving width is sufficiently narrow. Therefore, it is important to specify proper shallow groove pattern for stable winding at high speed with coated paper.

In this paper, it was intended to estimate the amount of air-entrainment at the nip and propose the proper grooving shape of nip roll in order to wind paper web stably at high speed. Nip profile along CD direction was estimated considering the deformation of surface layers of wound roll at grooved area. In the contact area, air film thickness was evaluated using the formula proposed by authors [3, 4]. In the no contact area at the bottom of grooves, air film thickness was evaluated considering the air pressure caused by web tension in CD direction. The effect of grooving shape of nip roll was evaluated from in-roll stress analysis with the consideration of the air-entrainment.

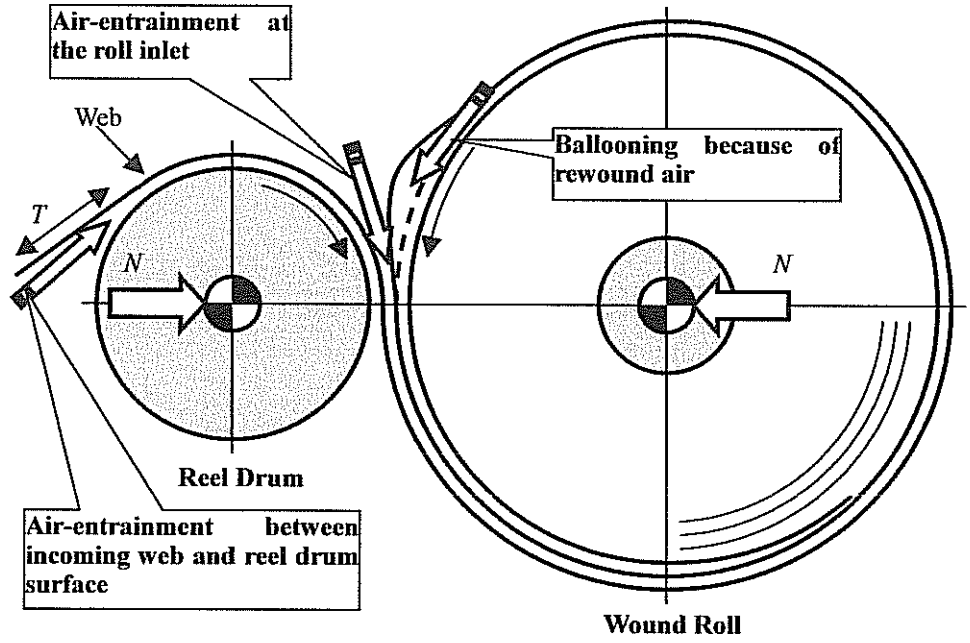

Fig. 1 Air-entrainment in winding system

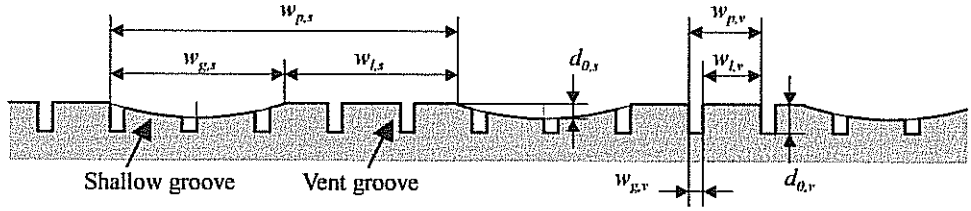

Fig. 2 Grooving geometry

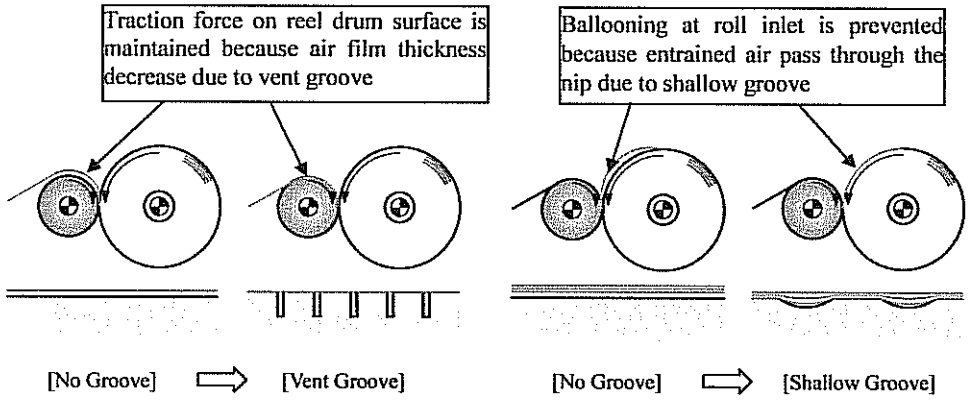

(a) Vent Groove (b) Shallow Groove

Fig. 3 Effect of grooves on nip roll surface

Air film thickness considering the effect of grooves

The numerical formulation of air-entrainment with no grooved nip roll was developed by Chang [8], authors [3, 4] and so on. On the other hand, it is unable to develop the strict formulation for estimating the air-entrainment with grooved nip roll without sophisticated knowledge about 3-dimensional fluid mechanics. We consider that it is not reasonable to develop the strict formulation for practical use. In this paper, we applied simple 2-dimensional model to estimation of air-entrainment considering the grooving shape.

Nip profile. First, nip profile at grooved area is calculated for estimating air-entrainment. Fig. 4 shows typical shape of shallow groove and coordinate system.

Nip contact width b is calculated by Hertz contact theory as follows;

$$b = \sqrt{\frac{4N}{\pi} C_{eq} R_{eq}} \qquad \{1\}$$

$$\text{Where, } C_{eq} = \frac{1-\nu_d^{\,2}}{E_d} + \frac{1-\nu_r^{\,2}}{E_r}, \quad R_{eq} = \frac{R_d R_r}{R_d + R_r} \qquad \{2\}$$

We assume that radial deformation of rolls was calculated from geometrical relationship as shown in Fig. 4.

$$\delta_0 = \delta_d + \delta_r = R_d(1-\cos\theta_d) + R_r(1-\cos\theta_r) \qquad \{3\}$$

$$\text{Where, } \theta_d = \sin^{-1}(b/R_d), \quad \theta_r = \sin^{-1}(b/R_r) \qquad \{4\}$$

Depth of groove in z direction $d(z)$ is calculated using δ_0, which is nip indention of wound roll at flat area, as follows;

$$\delta(z) = \begin{cases} \delta_0 - d(z) & for \quad \delta_0 > d(z) \\ 0 & for \quad \delta_0 \le d(z) \end{cases} \qquad \{5\}$$

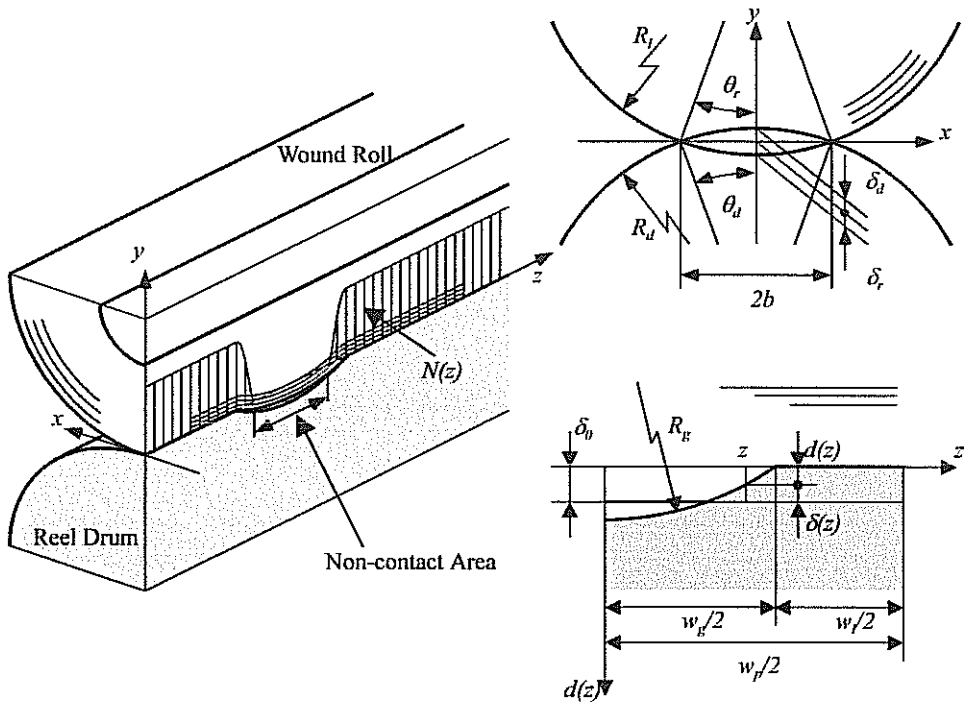

Fig. 4 Grooving geometry and roll deformation

Nip profile *N(z)* is obtained from eq. {1}~{5}, as follows;

$$N(z) = \frac{\pi b(z)^2}{4C_{eq}R_{eq}} \qquad \{6\}$$

Total nip force is obtained from integrating nip profile *N(z)* in z direction. Nip indention at flat area δ_0 is adjusted so that this total nip force correspond to applied nip force and final value of nip profile *N(z)* is obtained.

Air film thickness profile. Air film thickness profile in z direction is estimated 2 dimensionally and equivalent thickness is obtained as superposition of air film thickness in each position.

For estimating air film thickness in contact area, where *N(z)* > 0, the formula proposed by authors [3, 4] can be applied to estimate air film thickness. Air film thickness and nip pressure at the nip region is calculated by solving Reynolds equation with the consideration of elastic deformation of wound roll. Reynolds equation taking account of the compressibility of air, and the equilibrium equation with the nip load is shown in eq. {7} and {8}, respectively.

$$\nabla \cdot (ph^3 \nabla p) - 6\mu V \frac{\partial (ph)}{\partial x} = 0 \qquad \{7\}$$

$$\int_A p dA - N = 0 \qquad \{8\}$$

Air film thickness h is the sum of air film thickness at the nip center h_n, geometric clearance h_g and elastic deformation of wound roll δ_p as follows;

$$h = h_n + h_g + \delta_p \qquad \{9\}$$

In eq. {9}, elastic deformation δ_p is obtained using equivalent elastic modulus of wound roll surface layers and nip pressure p, of which values are calculated using the wound roll stress analysis method proposed by the authors [3, 4].

Nip pressure p and air film thickness h is obtained numerically with applying Newton-Raphson technique to solve eq. {7}, {8} and EHL equation with consideration of elasticity of wound roll.

On the other hand, in non contact area, where $N(z) = 0$, we applied the formula proposed by Good [9] and Hashimoto [7] as a trial. This formula was developed to evaluate air film thickness between running web and rotating roll. Theoretical value from this formula, however, resulted in over estimate compared with experimental value. Because this theory is based on foil bearing theory, axial tension of web is not considered and air film thickness is decided from circumferential tension and air pressure. In non-contact area of shallow groove, however, web float is strongly restricted by axial tension. it seems that axial tension of web in non-contact area was distributed by nip load at contact area. So, it was bold assumption but we assumed that web axial strain was obtained from geometrical relationship and air pressure calculated using web axial tension increment and curvature radius was equivalent to nip pressure in non-contact area. In accordance with above assumption, air film thickness in non-contact area can be estimated from eq. {7}, {8}.

Curvature radius of web in non-contact area is obtained from eq. {10}.

$$R_w = \frac{\Delta \delta_0}{2} + \frac{\Delta w_g^{\ 2}}{8 \Delta \delta_0} \qquad \{10\}$$

Where $\Delta\delta_0$ is web radial displacement caused by air pressure at the center of grooved area and Δw_g is width of non-contact area as shown in Fig. 5.

Therefore web axial strain ε_z and axial tension increment ΔT are calculated as follows;

$$\varepsilon_z = \frac{R_w \theta_w}{\Delta w_g / 2} - 1 \qquad \{11\}$$

$$\Delta T = t E_z \varepsilon_z \qquad \{12\}$$

Air pressure is obtained from eq. {10}, {12} as follows;

$$p = \frac{\Delta T}{R_w} \qquad \{13\}$$

Equivalent nip load $N_{non\text{-}contact}$ at non-contact area is obtained from air pressure p and Hertz contact theory as follows;.

$$N_{non-contact} = \pi C_{eq} R_{eq} p \qquad \{14\}$$

If web axial strain at non-contact area is affected with only air film thickness h, which is obtained from eq. {7}, {8} with use of nip load calculated by eq. {14}, web radial displacement $\Delta\delta_0$ is adjusted as follows;

$$\Delta\delta_0 = \frac{3}{2}h \qquad \{15\}$$

Equivalent nip load and air-film thickness at non-contact area are calculated from instituting web radial displacement from eq. {15} to eq. {10} ~ {14} iteratively.

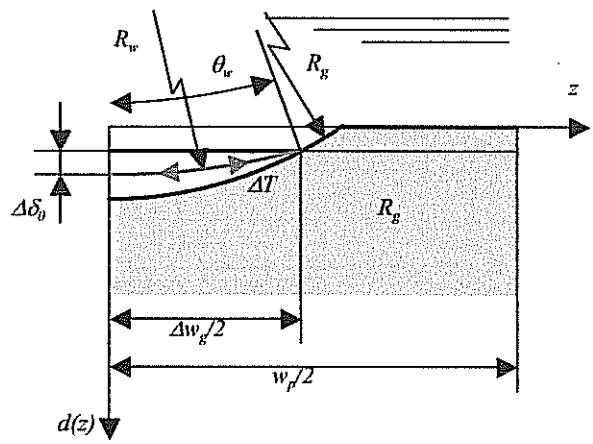

Fig. 5 Web deformation and tension increments at non-contact area

As identified above, air film thickness profile is obtained and the amount of air-entrainment is calculated by integrating air film thickness in axial direction (z direction). Equivalent nip load and air-film thickness at non-contact area are calculated from instituting web radial displacement from eq. {15} to eq. {10} ~ {14} iteratively.

It become to be able to estimate in-roll stress considering grooving shapes with applying above approach to in-roll stress analysis proposed by authors [3, 4].

EXPERIMENTAL VERIFICATIONS

Air film thickness considering Experimental procedure

Experimental set up and procedure. Air film thickness measurement tests were conducted by usage of small sized testing machine in order to assure the applicability of the proposed method. Fig. 6 shows the schematic figure of the testing machine. In general,

young modulus of nip roll surface is higher than that of wound roll surface because material of nip roll surface is metal or hard rubber in paper making machine. Therefore, in this testing machine, wound roll and nip roll should be modeled by soft rubber roll and metal roll, respectively. We chose material of soft rubber to make equivalent stiffness of two rolls equal to practical winding system. In order to evaluate air-entrainment into wound roll in practical winding system, we have to measure air film thickness on rubber roll in testing machine. It is, however, unrealistic to measure air film thickness at high accuracy within several μm orders because it seems to be difficult to make rubber roll circularity in several μm and air film thickness is predicted to be about several μm to several dozen μm. In addition, rubber roll is exposed to compressive stress repeatedly at the nip so that roll diameter increase with the effect of thermal expansion. For example, increase in roll radius is predicted to be 12 μm with 10 °C increase in temperature, in which it is assumed that linear expansion coefficient is 12×10^{-5} °C^{-1} and thickness of rubber is 10 mm. This thermal expansion of rubber roll is not negligible so that we changed the configuration of testing machine. In other words, nip roll was modeled by soft rubber roll with grooved and wound roll was modeled by metal roll.

In this testing machine, web curvature at the nip becomes opposite to practical winding system, but web curvature radius is sufficiently large compared with air film thickness. So, we consider that web curvature is negligible from the viewpoint of theory of lubrication. In addition, it is able to make metal roll circularity in 1 μm differently from rubber roll and displacement of metal roll surface is measurable with use of eddy-current sensor so that thermal expansion of metal roll can be corrected.

Specifications of testing machine are listed in Table 1. Metal roll axis is fixed and driven by motor. Rubber roll axis is applied load by air cylinder and then nip load is generated. Rubber roll was idle roll. Moving roll axis is applied load by air cylinder and web tension is generated. Web lateral motion of slide is controlled by crown and axis angle of paper roll. Two grooving rolls as the nip roll are prepared, in which one is vent groove and the other is combined grooves of vent and shallow grooves as listed in Table 2. Air film thickness is measured as the difference between radial displacement of web and that of metal roll as shown in Fig. 6.

Table 1 Specifications of testing machine

Item			Value
Web	Material	-	PET
	Width	W (mm)	200
	Thickness	t (μm)	50
	Young Modulus	E_w (MPa)	3.09×10^4
Metal Roll	Radius	R_m (mm)	100
	Width	W_m (mm)	230
Rubber Roll	Radius	R_r (mm)	100
	Width	W_r (mm)	230
	Rubber Thickness	h_r (mm)	20
	Rubber Hardness	H (°, JIS A)	50
Speed		V (m/min)	30~2000
Nip Load		N (kN/m)	0~5
Tension		T (kN/m)	0~0.3

Table 2 Grooving shape of small size test machine

Item			Value	
Rubber Roll No.			1	2
Shallow Groove	Depth	$d_{0.5}$ (mm)	0	1.4
	Width/Pitch	$w_{g.5}/w_{p.5}$ (-)	0	0.5
Venta Groove	Depth	$d_{0.v}$ (mm)	2.5	
	Width/Pitch	$w_{g.v}/w_{p.v}$ (-)	0.1	

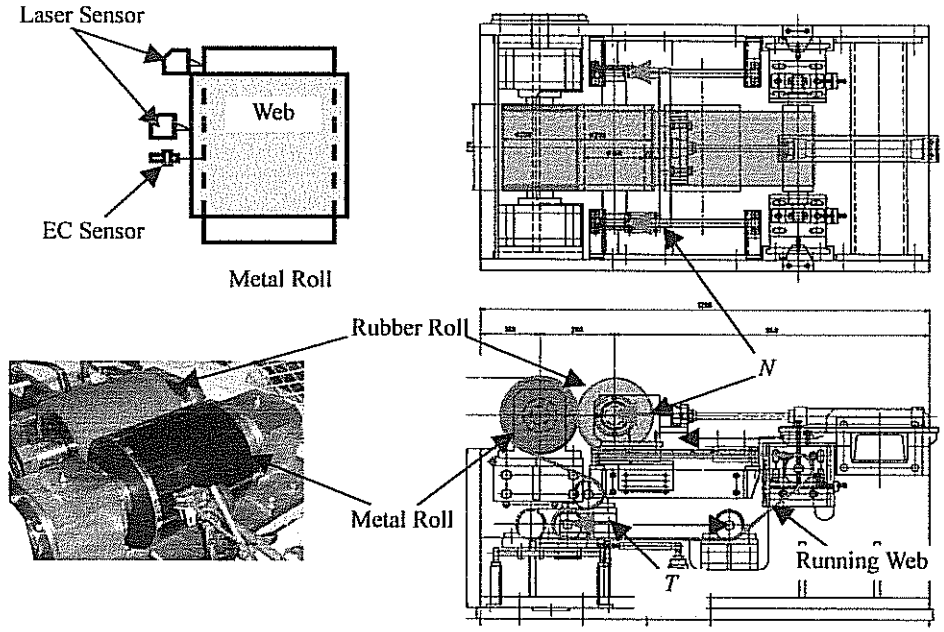

Fig. 6 Air film thickness testing machine

Experimental Results. Fig. 7 shows the comparison of the experimental results with the theoretical results of air film thickness for vent grooved nip roll. As is the case of vent grooved nip roll, Fig. 8 shows the comparison of the experimental results with theoretical results for combined grooved nip roll. In these tests, web running speed V was from 30 to 2000 m/min, nip load N was from 1 to 3 kN/m and web tension was 0.2 kN/m.

In the case of vent groove, both of the experimental and theoretical values of air film thickness increase with web running speed and decrease with nip load and the difference between the experimental results and the theoretical results is less than 2 μm under 1500 m/min as shown in Fig. 7. But experimental results of air film thickness increase suddenly over 1500m/min in web running speed and under 2 kN/m in nip load. We considered that this was because web running stability became into unstable state and flattering had occurred at low nip load.

In the case of combined grooves, both of the experimental and theoretical values of air film thickness increase with web running speed and decrease with nip load as shown in Fig. 8, as is the case of vent groove. It is remarkable that air film thickness with combined grooves is about 10 times larger than that with vent groove. We consider that this is because of excessive amount of air-entrainment at non-contact area of shallow

groove as above mentioned.

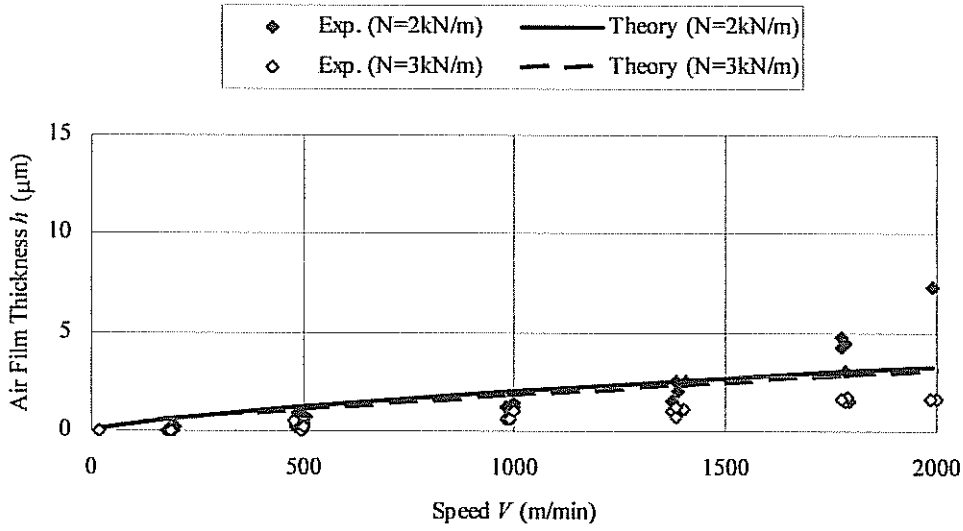

(a) Effect of web running speed

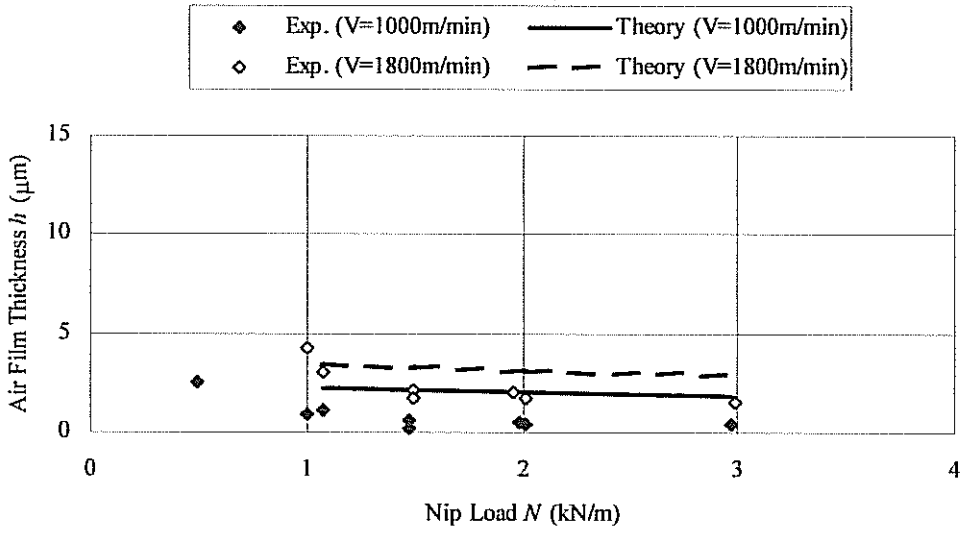

(b) Effect of nip load

Fig. 7 Air film thickness with rubber roll 1 (venta groove)

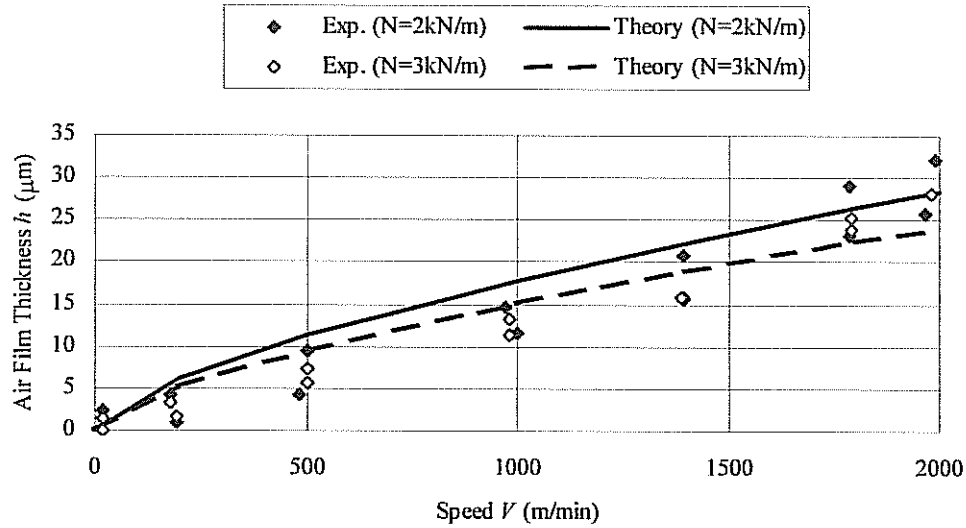

(a) Effect of web running speed

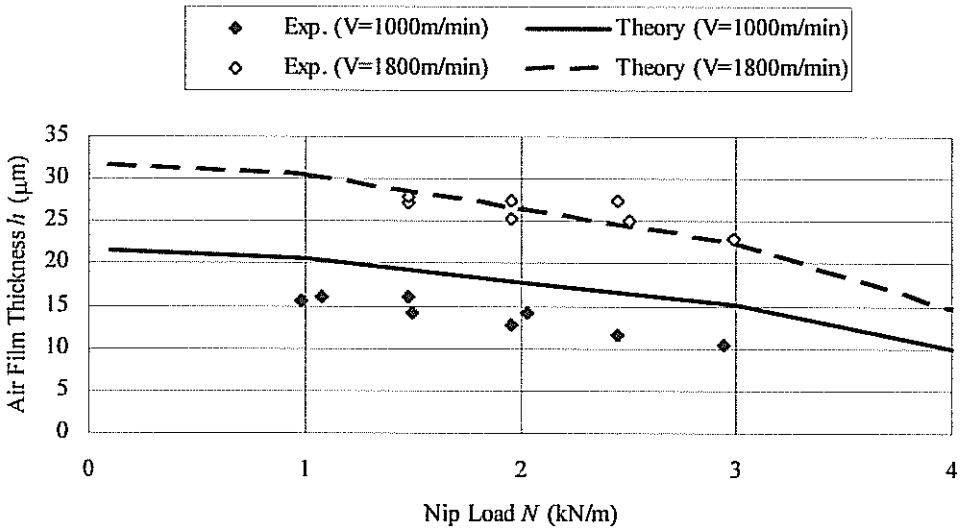

(b) Effect of nip load

Fig. 8 Air film thickness with rubber roll 2 (venta + shallow groove)

From experimental and theoretical investigations in this section, it is found that there are good agreements with experimental values and theoretical values of air film thickness considering the effect of grooving shape of nip roll surface.

In-roll stress of wound roll

Experimental procedure. In this section, winding tests were conducted by usage of our pilot reel in order to assure the applicability of the proposed method to in-roll stress analysis. Fig. 9 shows the schematic figure of our pilot reel. New wound roll is placed at the un-reel and the web is drawn out under the preset speed by the drag roll. Web tension is applied by the torque of both the nip roll and wound roll. Interlayer

pressure -σ_r is measured using FlexiForce™ in order to investigate the effect of grooving shape of nip roll surface. FlexiForce™ is a sensor that senses the change in resistance caused by the pressure in the wound roll. Sensors used in this test are calibrated beforehand by putting them in the stack of the same grade of paper and being loaded using the universal testing machine. These sensors are inserted in the paper sleeves and are pasted at the both of the web in advance.

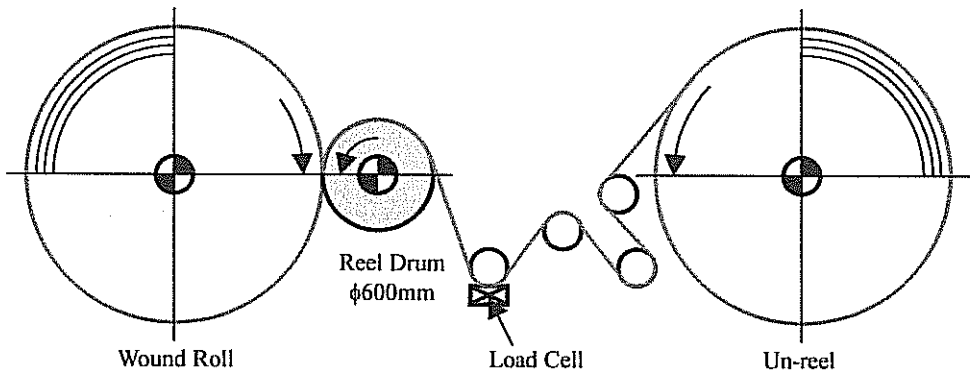

Fig. 9 Test reel

Test Conditions. Specifications of testing machine and winding parameters are listed in Table 3. Three grooving nip rolls are prepared in order to evaluate the effect of grooving depth of shallow groove. Grooving shapes of nip roll are listed in Table 4. Coated paper is prepared for winding tests. Material properties of coated paper are listed in Table 5.

Table 3 Specifications of test reel and winding parameters

Item			Value
Wound Roll	Radius	R_r (mm)	685 (Max. 1000)
	Width	W_r (mm)	765
Reel Drum	Radius	R_d (mm)	600
	Width	W_d (mm)	900
Core	Radius	R_c (mm)	220
	Width	W_c (mm)	900
Speed		V (m/min)	30~2000 (Max. 3000)
Nip Load		N (kN/m)	2.5 (Max. 10)
Tension		T (kN/m)	0.4 (Max. 1.0)

Table 4 Grooving shape of test reel

Item			Value
Shallow Groove	Depth	$d_{0.5}$ (mm)	0, 0.25, 0.75
	Width/Pitch	$w_{g.s}/w_{p.s}$ (-)	0.5
Venta Groove	Depth	$d_{0.v}$ (mm)	2.5
	Width/Pitch	$w_{g.v}/w_{p.v}$ (-)	0.1

Table 5 Material properties of paper

Item		Value
Paper Grade		Coated paper
Thickness t (μm)		57.7
Young Modulus	E_θ (MPa)	7.30×10^3
	E_z (MPa)	3.64×10^3
	E_r (MPa)	$A=7.30\times10^4$, n=3.37 ($-\sigma_r = A\varepsilon_r^n$)
Coefficient of air permeance β (m/sec/Pa) (Permeability (sec))		7.94×10^{-9} (15,105)
Frictional Coefficient μ_{st} (-)	Paper / Paper	0.40
	Paper / Reel Drum	0.42
Surface Roughness $R_{q\,web}$ (μm)		0.37

Experimental Results. Fig. 10 shows the comparison of experimental and theoretical results of interlayer pressure $-\sigma_r$ for each grooving depth listed in Table 4. The winding speed of 2000 m/min is achieved from the radius of 400 mm.

Fig. 10(a), (b) and (c) shows the effect of the depth of shallow groove. It is found that interlayer pressure decrease with grooving depth from experimental and theoretical values. We think that this is because increase in air-entrainment with grooving depth makes radial stiffness of wound roll become lower and therefore increments of radial stress is decreased.

We make sure that interlayer pressure of wound roll considering the effect of grooving shape can be estimated by the proposed method and in-roll stress analysis proposed by authors [3, 4]. So, it become to be able to design the proper winding system without roll defects, lateral slide or interlayer slippage and so on, caused by excessive entrained air considering the effect of grooving shape of nip roll surface and many winding parameters in winding system.

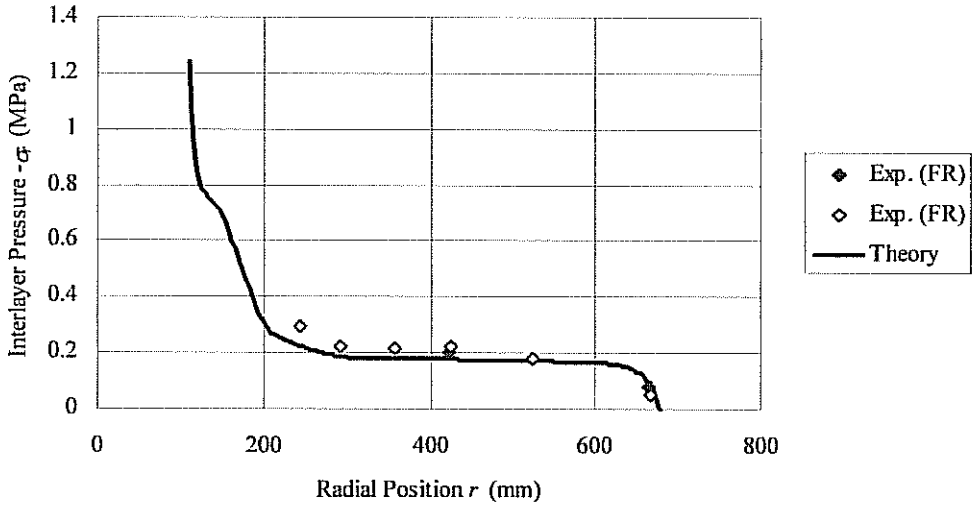

(a) Vent groove

Fig. 10 In-roll stress of wound roll

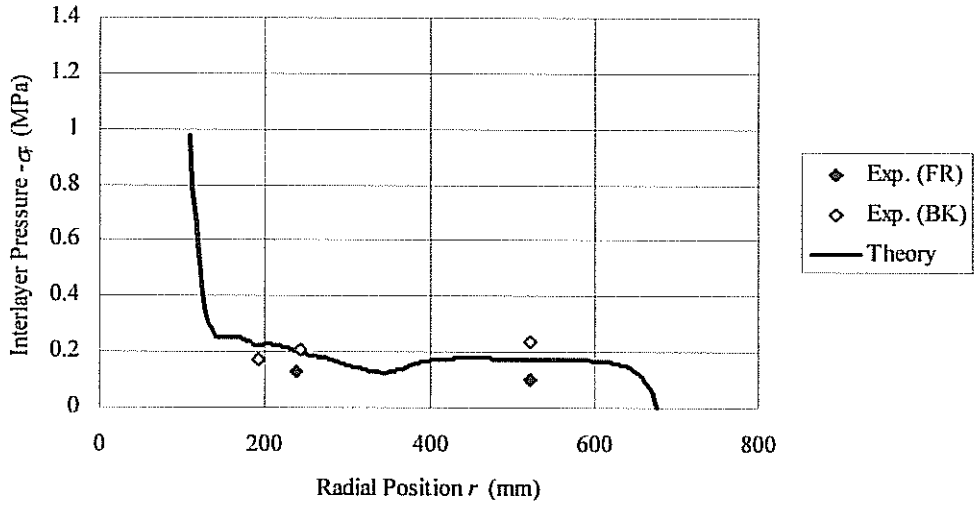

(b) Vent + Shallow groove ($d_{0,s}$=0.25mm)

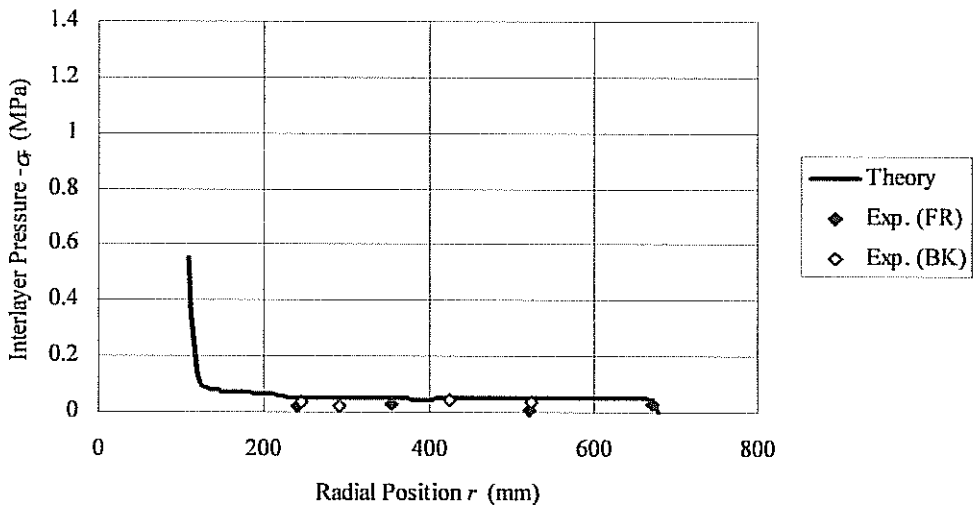

(c) Vent + Shallow groove ($d_{0,s}$=0.75mm)

Fig. 10 In-roll stress of wound roll

CONCLUSIONS

The authors proposed a simple method for evaluating the effect of grooving shape of nip roll surface on air-entrainment at the nip and applied this method to estimate in-roll stress of wound roll. Air film thickness and in-roll stress fields were examined theoretically and experimentally and they showed the significant effect of grooving shape upon air film thickness and in-roll stress.

Consequently, we found that it became to be able to propose the optimal shape of grooves on nip roll surface to maintain the stable winding at high speed and at large-diameter in practical winding system.

REFERENCES

1. Altmann, H. C., "Formulas for Computing the Stresses in Center-Wound Rolls", Tappi Journal, Vol. 51, No. 4, 1968, pp. 176-179.
2. Hakiel, Z., "Nonlinear Model for Wound Roll Stresses", Tappi Journal, Vol. 70, No. 5, 1987, pp. 113-117.
3. Tanimoto, K., Kohno, K., Sasaki, M., Michiura, K., "In-roll Stress Analysis of Wound Roll with the Air Entrainment and the Permeation", Proceedings of the Sixth International Conference on Web Handling, Web Handling Research Center, Stillwater, Oklahoma, 2001.
4. Tanimoto, K., Kohno, K., Takahashi, S., Sasaki, M. and Yoshida, F., "Numerical Stress Analysis of Wound Roll with Air-Entrainment", Transaction of the JSME, Vol. 68-665 A, 2002, pp. 161-168.
5. Tanimoto, K., "Traction Force Between Rotating Roll and Moving Web Considering the Effect of Air-entrainment and Friction", Proceedings of the Seventh International Conference on Web Handling, Web Handling Research Center, Stillwater, Oklahoma, 2003.
6. Good, J. K., Kedl, D. M. and Shelton, J. J., "Shear Wrinkling in Isolated Spans", Proceedings of the Fourth International Conference on Web Handling, Web Handling Research Center, Stillwater, Oklahoma, 1997, pp. 462-480.
7. Hashimoto, H., "Triborogical Approach to Web Handling Problems", Proceedings of the JSME, Vol. 1999, No. 5, 1999, pp. 183-184.
8. Chang, Y. B., Chambers, F. W. and Shelton, J. J., "Elastohydrodynamic Lubrication of Air-Lubricated Rollers", Journal of Tribology, Transaction of the ASME, Vol. 118, 1996, pp. 623-628.
9. Ducotey, K. S., Good, J. K., "The Effect of Web Permeability and Side Leakage on the Air Film Height Between a Roller and Web," Transaction of the ASME, Journal of Tribology, Vol. 120, 1998, pp. 559-565.

In-Roll Stress Analysis Considering Air Entrainment at the Roll Inlet with the Effect of Grooves on the Nip Roll Surface

M. Sasaki[1], K. Kohno[1], K. Tanimoto[1], S. Takahashi[1], S. Suzuki[1] & H. Hashimoto[2], [1]Mitsubishi Heavy Industries, Ltd. & [2]Tokai University, JAPAN

Name & Affiliation	Question
Gabriela Simbierowicz Metso Paper	I would like to ask you about the depth of these shallow grooves. Was that increased by 0.25 millimeters? Both 0.25 and 0.75 mm. Did you make any calculations with smaller steps between 0 and 0.25 millimeters because these differences are pretty large.
Name & Affiliation	**Answer**
Koshi Tanimoto Mitsubishi Heavy Industries, Ltd.	I tried these with 0.25 and 0.75 mm.
Name & Affiliation	**Question**
Gabriela Simbierowicz Metso Paper	Do you think the air entrapment is smaller when you have, for example, 0.1 millimeter?
Name & Affiliation	**Answer**
Koshi Tanimoto Mitsubishi Heavy Industries, Ltd.	I haven't tried it.
Name & Affiliation	**Question**
Dave Roisum Finishing Technologies, Inc.	They have a similar groove that they use in the converting industry. They call it a burping groove for almost identical purposes. But they do it quite differently than the paper industry. In the paper industry, the pitch is a couple inches; in the converting industry, it is a couple feet. It only needs one chance per revolution and the more area of groove you have, the more air goes in. Have you investigated pitch?
Name & Affiliation	**Answer**
Koshi Tanimoto Mitsubishi Heavy Industries, Ltd.	I haven't examined pitch. We have only examined the depths.